

Corticostriatal Activity Driving Compulsive Reward Seeking

Masaya Harada, Vincent Pascoli, Agnès Hiver, Jérôme Flakowski, and Christian Lüscher

ABSTRACT

BACKGROUND: Activation of the mesolimbic dopamine system is positively reinforcing. After repeated activation, some individuals develop compulsive reward-seeking behavior, which is a core symptom of addiction. However, the underlying neural mechanism remains elusive.

METHODS: We trained mice in a seek-take chain, rewarded by optogenetic dopamine neuron self-stimulation. After compulsivity was evaluated, AMPA/NMDA ratio was measured at three distinct corticostriatal pathways confirmed by retrograde labeling and anterograde synaptic connectivity. Fiber photometry method and chemogenetics were used to parse the contribution of orbitofrontal cortex afferents onto the dorsal striatum (DS) during the behavioral task. We established a causal link between DS activity and compulsivity using optogenetic inhibition.

RESULTS: Mice that persevered when seeking was punished exhibited an increased AMPA/NMDA ratio selectively at orbitofrontal cortex to DS synapses. In addition, an activity peak of spiny projection neurons in the DS at the moment of signaled reward availability was detected. Chemogenetic inhibition of orbitofrontal cortex neurons curbed the activity peak and reduced punished reward seeking, as did optogenetic hyperpolarization of spiny projection neurons time-locked to the cue predicting reward availability.

CONCLUSIONS: Our results suggest that compulsive individuals display stronger neuronal activity in the DS during the cue predicting reward availability even when at the risk of punishment, nurturing further compulsive reward seeking.

<https://doi.org/10.1016/j.biopsych.2021.08.018>

Repeated activation of the mesolimbic dopamine system is reinforcing and may trigger compulsive behavior. Compulsive drug seeking is a hallmark of addiction (1) with deleterious consequences on physical, social, and economic well-being. While addictive drugs are widely used recreationally, only a small fraction of individuals lose control over drug intake (2). Individual differences in vulnerability to addiction have also been observed in laboratory animals (3–5), using models that apply punishment as a noxious electrical foot shock (6) or in the form of an aversive, bitter taste for oral self-administration (7). Across different drug self-administration schedules and with multiple classes of addictive drugs, compulsion is observed in a fraction of animals (3,7–9). Here, we define compulsion as the perseverance of self-administration in the presence of punishment.

We focus on compulsive reward seeking, reflecting the incapacity to shift from habitual to goal-directed motivational control (10), which may involve distinct neural substrates and cognitive strategies compared with compulsive reward-taking behavior (6). In rodents, compulsive drug seeking can be modeled by using a seek-take chain schedule of cocaine self-administration that includes a random time interval, after which the animal has to press a seek lever once more to gain access to the take lever. After the acquisition, an aversive stimulus is

delivered to the seek lever instead of the take lever in a fraction of trials.

During the early stage of addiction, drug-evoked dopamine (DA) transients in the nucleus accumbens (NAc) positively reinforce self-administration (11,12). Resulting dopamine-dependent synaptic plasticity in the NAc and the ventral tegmental area (VTA) have been causally linked to drug-adaptive behaviors, including locomotor sensitization and cue-associated seeking behavior (13–17). At later stages of drug exposure, transition to compulsive drug use may be mediated by the recruitment of potentiated synapses in more dorsal areas of the striatum (1,18). The dorsal striatum (DS), which is also the site of habit formation (19,20), may therefore play a role in the incapacity to shift from habitual to goal-directed behavior, which defines compulsive drug seeking. Consistent with this hypothesis, pharmacological inhibition of the dorsolateral striatum reduces compulsive drug-seeking behavior (21) and habitual drug seeking (20).

Top-down control of the striatum arises in the anterior cortex, where neurons of the medial prefrontal cortex (mPFC), orbitofrontal cortex (OFC), and primary motor cortex (M1) send their axons to subregions of the DS. The striatum, subdivided into the dorsolateral, dorsomedial, and ventral striatal regions, is functionally associated with sensorimotor, associative, and

SEE COMMENTARY ON PAGE 800

limbic processes, respectively (22–27). The three main projections to the DS (28) (mPFC to dorsomedial, OFC to central, and M1 to dorsolateral striatum) may all be implicated in compulsive reward seeking, but their respective role remains elusive. Contrasting mPFC hypofunction and OFC hyperfunction both may favor the appearance of compulsion (5,29–31). The motor cortex, believed to control habitual responding via its projection to the dorsolateral striatum, may be involved in compulsive drug seeking if there is a failure to disengage habitual behavior (32).

It remains unknown how pathway-specific activity patterns and synaptic plasticity emerging after drug self-administration reinforce drug seeking despite negative consequences. To tackle these questions, we implemented optogenetic DA neuron self-stimulation (oDASS) in the VTA in a seek-take chained schedule. Because all addictive drugs induce their reinforcing effects by elevating DA in the NAc (11,12), this oDASS allows us to focus on mechanisms common to several addictive drugs while avoiding off-target effects of individual substances. Moreover, oDASS evokes analogous plasticity to cocaine in the VTA (33) and NAc (5) and results in a dissociation between punishment-sensitive and punishment-resistant phenotypes (5,29). To probe for compulsive reward seeking, we tested whether mice would persevere in the seek-take chain despite having to endure a foot shock. We found that this behavior was bimodally distributed, with about 60% of the mice fulfilling the criterion for compulsive reward seeking. Combining circuit tracing, ex vivo assessment of synaptic transmission, photometry, and chemogenetic and optogenetic manipulations, we revealed a critical involvement of OFC-DS projections in compulsive seeking behavior. We identified a peak in spiny projection neuron (SPN) activity at the moment of seek lever retraction, which may lead the animal to engage in subsequent trials, thus providing a cellular explanation for compulsive seeking.

METHODS AND MATERIALS

See [Supplemental Methods and Materials](#) for extended details.

We used DAT-Cre mice following a protocol approved by the institutional, cantonal, and federal authorities to inject viral vectors (AAV5 and 8) to express either floxed versions of channelrhodopsin-2 (ChR2) or Chrimson in DA neurons of the VTA (anterior-posterior -3.3 ; medial-lateral -0.9 with a 10° angle; dorsal-ventral -4.28). We also used cholera-toxin subunit B-conjugated fluorophores for anatomical tracing.

The mice then had the opportunity to self-stimulate using a modified operand chamber (MED Associates) to implement a seek-take chain after initial training of 5 days in a simple taking response (oDASS). The mice pressed the seek lever during a duration unknown to the animal (random interval of 45, 60, or 75 s), after the end of which the press on the seek lever resulted in the delivery of the take lever. Once the performance was stable, we introduced an electric shock (0.25 mA, 500 ms) at the last seeking press. Compulsion was assessed by using a clustering algorithm on 5 key behavioral parameters.

Electrophysiology was carried out in acute slices to measure the amplitudes of excitatory postsynaptic currents (EPSCs) in voltage-clamp configuration. AMPA and NMDA

EPSCs were pharmacologically isolated to calculate a ratio reflecting synaptic strength. Opto- and chemogenetic interventions were also validated in brain slices by wide-field illumination or bath application of clozapine N-oxide (CNO), respectively.

In vivo fiber photometry to report activity using a fluorescent calcium indicator (AAV5-CaMKII-GCaMP6f) was carried out in parallel with oDASS using 2 spectrally separated optogenetic effectors. The injection site was verified post hoc.

The analysis used a standard statistical test in GraphPad Prism (GraphPad Software, Inc.) and a hierarchical clustering method (MATLAB [The MathWorks, Inc.] functions `pdist`, `linkage`, `cluster` with a squared Euclidean metric and ward linkage distance) to identify persevering individuals.

RESULTS

Compulsive oDASS Seeking in a Fraction of Mice

We injected the VTA of DAT-Cre mice with an AAV5-EF1a-DIO-ChR2-eYFP and implanted an optic fiber just above the injection site (Figure 1A). Two weeks later, mice first acquired a taking response and then were trained under a seek-take chain for an unpredictable interval (Figure 1B, C), after which they had to press the seek lever once more to access the take lever (see [Methods and Materials](#) for details). All mice completed 30 trials (random interval = 60 s) in 4 daily baseline sessions (Figure 1F, G). The mice then underwent 5 days of punished sessions, during which a foot shock was delivered with the first press on the last seek lever in 30% of the trials (Figure 1B, D). This schedule caused some mice to stop pressing on the seek lever (Figure 1F; Figures S1 and S2). Using an unsupervised classification method, 2 distinct groups of mice emerged (Figure 1G; Figure S2). About 40% reduced their seeking behavior and were unable to complete most of the trials under punishment, which we called renouncers. The second group, called perseverers, about 60% of all mice, maintained seek lever pressing under punishment and completed most trials (Figure 1G). The number of seek lever presses during the baseline sessions was not different between the two groups and thus not predictive of perseverance (Figure 1H; Figure S2). Overall, the fraction of completed trials was reduced during punished sessions for renouncers but not perseverers. Histological verification confirmed that there was no difference in the expression of ChR2 in the VTA (Figure S3). We next tested for cue-induced reinstatement, an established model of relapse (34,35). After punished oDASS sessions, mice were retrained on the take lever alone (Figure S4), followed by extinction sessions where presses on the take lever no longer resulted in laser stimulation or cue light presentation. Mice then underwent a reinstatement session whereby take lever presses triggered the cue light presentation without laser stimulation. This led to an increase in take lever presses, indicating that oDASS evokes behavioral adaptations similar to addictive drugs (Figure S4).

Parallel Corticostriatal Streams

To probe the underlying neural circuits, we characterized corticostriatal projections (28). We injected retrograde tracers of distinct colors into the medial, central, and lateral parts of

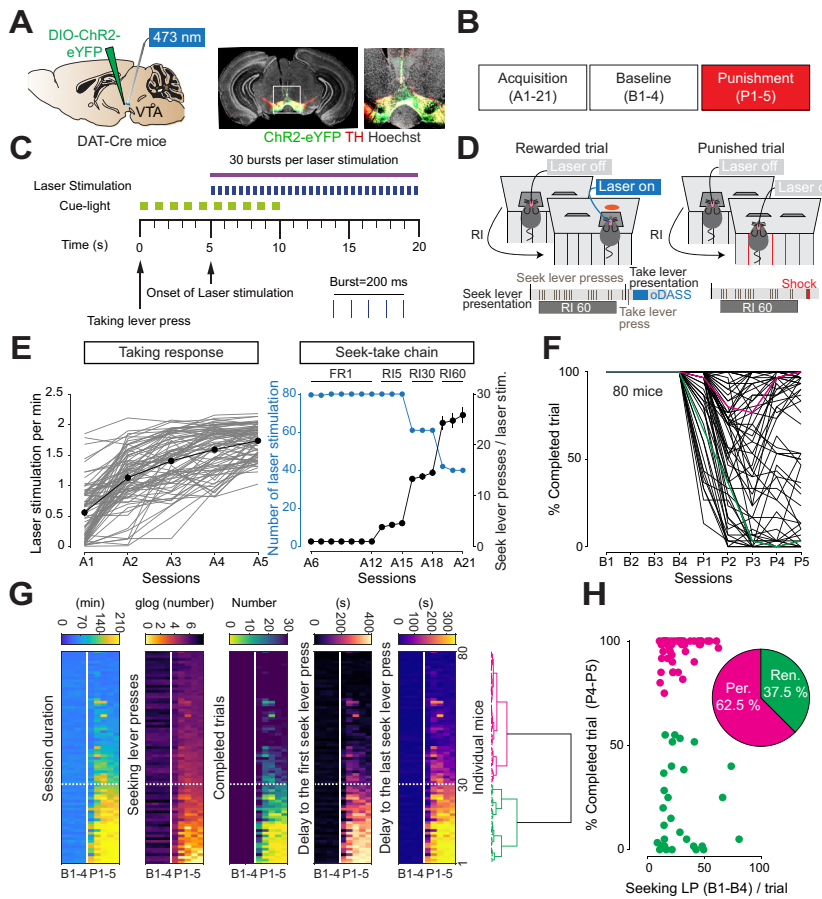


Figure 1. oDASS seeking despite negative consequences in a subset of mice. **(A)** Schematic of optic fiber implantation into the VTA of DAT-Cre mice (left) infected with AAV5-EF1 α -DIO-ChR2-eYFP and staining of tyrosine hydroxylase (middle and right). **(B)** Experimental timeline. **(C)** Schematic for the laser stimulation. Pressing on the take lever triggers the cue light delivery, followed by the laser stimulation 5 seconds later. **(D)** During rewarded trials, the first seek lever press after the end of the RI triggered the retraction of the seek lever and the presentation of the take lever. A single press on the take lever resulted in the delivery of the laser stimulation. During punished trials, the first seek lever press after the end of RI triggered the retraction of the seek lever and the delivery of the foot shock (500 ms, 0.25 mA, right). **(E)** Acquisition of seek-take chained schedule for oDASS (A1-21). During taking response training, only the take lever was presented with the seek lever retracted. Single press on the take lever triggered the laser stimulation (left). After 5 sessions of taking response training, acquisition sessions of seek-take chained schedule started (right). **(F)** Percent of completed trials during baseline (4 days) and punished (5 days) sessions. Green and pink lines identify the example of 2 mice shown in Figure S1. During baseline sessions, all trials were rewarded. During punishment sessions, 70% of the trials were still rewarded and the other 30% of the trials were punished. **(G)** The unsupervised clustering method yields 2 clusters (Ren. and Per.). **(H)** Percent of completed trials as a function of the number of seek lever presses per trial during baseline sessions. oDASS, optogenetic dopamine neuron self-stimulation; LP, lever press; Per., perseverer; Ren., renouncer; RI, random interval; VTA, ventral tegmental area.

the DS (mDS, cDS, and IDS, respectively) (Figure 2A, B; Figure S5). With seeding in the mDS, we observed cell bodies retrogradely labeled predominantly in the mPFC, especially within the prelimbic cortex and anterior cingulate cortex (Figure 2C, D; Figures S5 and S6). With the injection in the cDS, we retrogradely labeled neurons in the OFC, frontal association cortex, and secondary motor area (Figure 2C, D; Figure S5). Finally, with injections in the IDS, cells in the frontal association cortex, secondary motor area, M1, and primary somatosensory cortex were filled (Figure 2C, D). Some cells were colabeled with more than one dye in frontal association cortex and secondary motor area (Figure 2C, D; Figures S5 and S6), indicating that some pyramidal neurons have collateral. By and large, however, neurons in the prelimbic cortex, anterior cingulate cortex, OFC, M1, and primary somatosensory cortex project to subregions of the DS with only a few collaterals. To demonstrate synaptic transmission, we next injected the anterograde tracer AAV8-hSyn-ChrimsonR-tdTomato in the mPFC, OFC, or M1 (Figure 3A), yielding fibers in the respective subregions of the DS (Figure 3B). Selective optogenetic activation in acute brain slices produced large light-evoked EPSCs in SPNs of the mDS, cDS, and IDS, respectively (Figure 3C), again with only limited mixed inputs found in DS subregions most likely

without cell-type specificity. OFC projects to both D1- and D2-SPNs with similar connectivity rates and amplitudes (36). Taken together, our functional and anatomical investigations confirm the existence of largely nonoverlapping cortico-striatal projections.

Enhanced Transmission in Corticostriatal Synapses of Compulsive Mice

Next, we assessed the synaptic strength of the three corticostriatal streams *ex vivo* in mice that underwent punished oDASS seeking. To selectively elicit glutamate release, we expressed the red-shifted excitatory opsin ChrimsonR in the mPFC, OFC, or M1 of DAT-Cre mice infected with ChR2 in the VTA (Figure 4A, C, E) and prepared acute slices 24 hours after the last punished session. Because previous results did not show any difference between D₁ receptor- and D₂ receptor-SPNs in synaptic strength in the DS (29) and both populations are activated by acute cocaine injection (36), our experiments were done without SPN subtype distinction. We calculated the AMPA receptor-EPSCs to NMDA receptor-EPSCs ratio (A/N) at positive potential (+40 mV, using pharmacological isolation). We found that the A/N ratio at OFC-cDS was higher in slices from persevering mice than in slices from

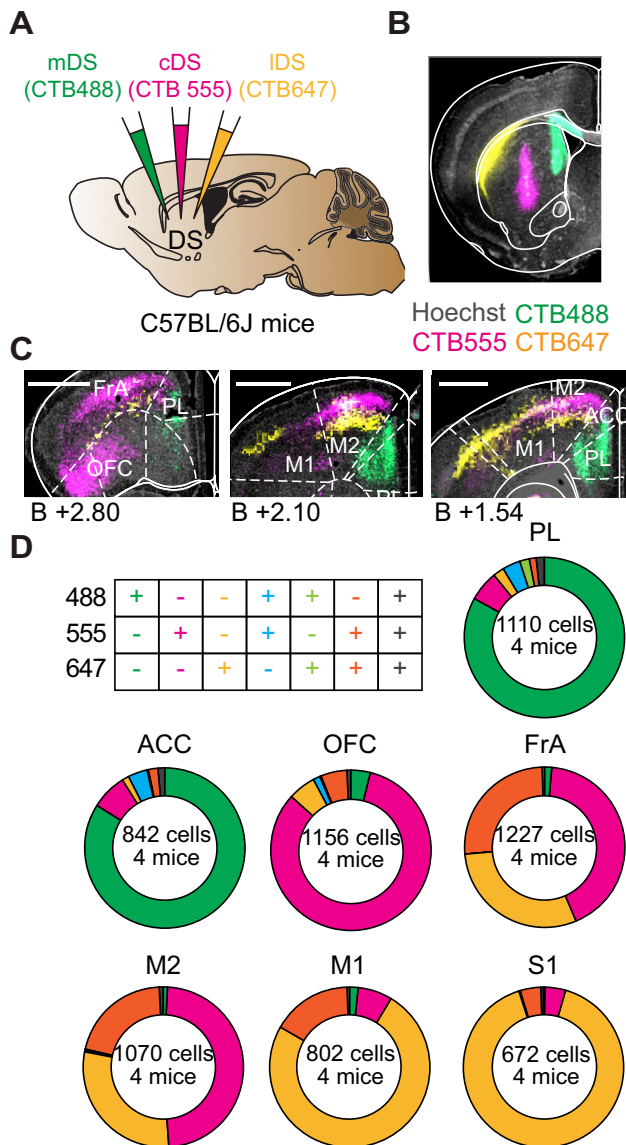


Figure 2. Three parallel corticostriatal pathways. **(A)** Schematic for the experiment. **(B)** Retrograde tracer CTB conjugated to the dye Alexa 488 (green), 555 (pink), or 647 (yellow) was injected in the medial, central, or lateral part of the DS, respectively. **(C)** Example pictures taken from the cortex. **(D)** Quantification in the PL, ACC, OFC, FrA, M2, M1, and S1 for each striatal projection. Scale bars = 1 mm. ACC, anterior cingulate cortex; cDS, central part of the dorsal striatum; CTB, cholera-toxin subunit B; DS, dorsal striatum; FrA, frontal association cortex; lDS, lateral part of the dorsal striatum; M1, primary motor cortex; M2, secondary motor cortex; mDS, medial part of the dorsal striatum; OFC, orbitofrontal cortex; PL, prelimbic cortex; S1, primary somatosensory cortex.

renouncing or naïve mice (Figure 4D), while at mPFC-mDS and M1-IDS synapses, the A/N ratios in persevering, renouncing, and naïve mice were not different (Figure 4B, F). Of note, the A/N ratio was smaller at M1-IDS than at the other synapses in all 3 groups of mice. Taken together, these data demonstrate that strength was selectively increased in compulsive mice at OFC-cDS synapses. We also measured the rectification index at

these three corticostriatal pathways, detecting no differences between groups (Figure S7).

Activity Peak at Seek Lever Retraction in Persevering Mice

We next asked whether synaptic potentiation could alter neural activity in vivo. To this end, we monitored intracellular calcium as a proxy for neural activity, expressing AAV5-CaMKII-GCaMP6f in the cDS and recording fluorescence with optic fibers (Figure 5A). To spectrally separate the calcium signal from oDASS, we used AAV8-hSyn-DIO-ChrimsonR-tdTomato for oDASS (Figure 5A). During baseline sessions, a robust calcium peak was detected after the seek lever retraction in both perseverers and renouncers (Figure 5B, C), albeit with an amplitude that was higher in mice later identified as perseverers (Figure 5C). Aligned to seek lever extension, seek lever press, take lever press, or laser stimulation, a much smaller increase in calcium signal was detected (Figure S8). Because the take lever was presented shortly after the seek lever retraction (Figure 5B), the signal could mainly result from take lever presentation. Therefore, in a separate experiment, we extended the interval between the two levers' movements to 3 seconds (Figure S9) and found that peak calcium activity coincided with the retraction of the seek lever (Figure S9). During punishment sessions, the calcium signal at seek lever retraction was still observed in persevering mice but disappeared in renouncers (Figure 5D). To compare this reduction in the two experimental groups, the peak amplitude around seek lever retraction during the punishment session was normalized to the peak amplitude during baseline sessions, showing the reduction of peak amplitude specifically in renouncers (Figure 5E). As a control experiment, we aimed the fiber at the lateral part of the DS (Figure S10), where we did not detect any difference in calcium signal around seek lever retraction (Figure S10), seek lever presentation, seek lever press, take lever press or laser stimulation (Figure S11). This is consistent with ex vivo electrophysiology data (Figure 4F; Figure S7). Taken together, the retraction of the seek lever caused a peak of activity, which was also observed during punishment sessions in perseverers, while in renouncers the calcium signal declined during punishment sessions. This was only observed in the central part of the DS, the preferred target region of OFC neurons, which also undergo synaptic strengthening.

OFC Inhibition During Compulsive oDASS Seeking

We next expressed the inhibitory DREADD (designer receptor exclusively activated by designer drugs: CaMKIIa-hM4D) in the OFC (Figure 6A, C). To validate the chemogenetic approach, we evoked OFC-DS transmission and bath-applied CNO (10 μM) to acute DS slices of mice infected with both hM4D and Chrimson in the OFC. CNO reduced optogenetically evoked EPSCs recorded from SPNs (Figure 6B), most likely by preventing glutamate release from OFC terminals (37). Next, to silence the OFC during behavior, we injected AAV1-CaMKII-hM4D-mCherry in the OFC and AAV8-hSyn-DIO-ChrimsonR-tdTomato in the VTA of DAT-Cre mice. In addition, AAV5-CaMKII-GCaMP6f was injected into the cDS and an optic fiber was positioned to allow photometry

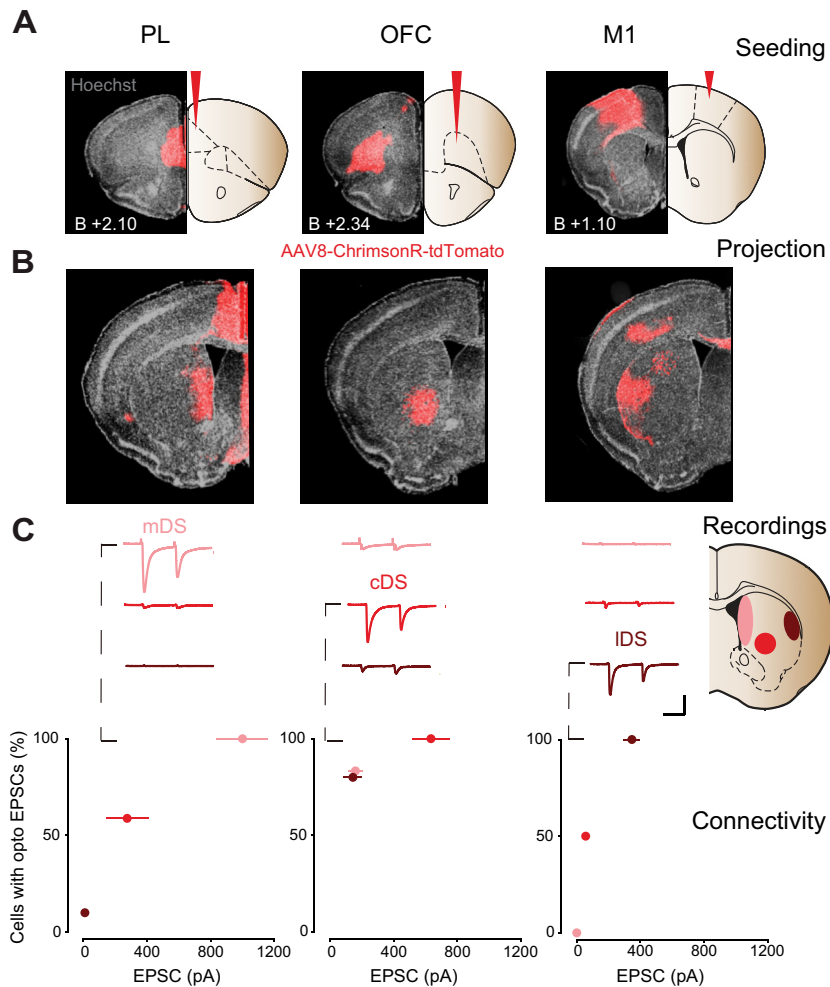


Figure 3. Synaptic connectivity at parallel corticostriatal pathways. **(A)** Coronal images of mice brain slices infected with AAV8-hSyn-ChrimsonR-tdTomato in the PL (left), OFC (center), and M1 (right). **(B)** Coronal images of the dorsal striatum corresponding to the images of **(A)**. **(C)** Synaptic connectivity between the PL (left), OFC (middle), and M1 (left) and DS subregions. EPSCs were recorded in the medial (light red), central (red), and lateral (dark red) part of the striatum. Number of recorded neurons (medial/central/lateral): PL, 12/17/10; OFC, 12/12/10; M1, 12/12/12. Scale bars = 50 ms, 500 pA. Error bars, SEM. cDS, central part of the dorsal striatum; EPSC, excitatory postsynaptic current; IDS, lateral part of the dorsal striatum; M1, primary motor cortex; mDS, medial part of the dorsal striatum; OFC, orbitofrontal cortex; PL, prelimbic cortex.

recording of SPN activity in response to chemogenetic OFC inhibition (Figure 6C). CNO injected 1 hour before the recording session (2 mg/kg, intraperitoneal) attenuated the calcium peak at seek lever retraction (Figure 6D). This experiment was conducted only in persevering mice previously selected during additional punished sessions. Finally, chemogenetic inhibition of the OFC of persevering mice was sufficient to reduce the number of completed trials during punished sessions (Figure 6E). The relative reduction of completed trials was proportionate to the attenuation of the calcium peak (Figure 6F). Histological verification indicated the expression of CaMKII-hM4D-mCherry in all mice (Figure S12). In the absence of hM4D expression, CNO had no impact on calcium activity in the cDS or compulsive reward seeking (Figure 6D, E). Because no differences in synaptic transmission were observed in the PFC-mDS or M1-IDS pathways, chemogenetic inhibition was performed only in the OFC. Taken together, these data indicate that the activity of SPNs at seek lever retraction was driven by excitatory inputs from the OFC, which, when inhibited, reduced compulsive seeking for oDASS.

Time-Locked Inhibition of SPN Activity

To probe the exact timing of the OFC-DS activity required, we next inhibited SPNs time-locked to the seek lever retraction. To this end, we injected AAV5-CaMKII-eArchT3.0-eYFP in the cDS and placed optic fibers bilaterally (Figure 7A, B). In acute slices, orange light (wavelength; 585 nm) activated ArchT3.0 and effectively suppressed action potentials induced by a depolarizing current injection (Figure 7C). First, mice underwent 5 sessions of punished oDASS to identify perseverers. Next, 9 additional punished sessions were performed with or without inhibition of cDS SPNs (shown as test and control, respectively) for 4 seconds starting at the first seek lever press after the end of random interval to silence SPNs during the seek lever retraction (Figure 7D, top). Compulsive seeking parameters were reduced by the time-locked cDS inhibition but recovered quickly in sessions without inhibition (Figure 7D, F). This inhibition at seek lever press did not affect seeking in baseline conditions (Figure S13). Moreover, applying optogenetic inhibition at the first seek lever press of each trial (Figure 7E, top), when only small calcium transients were observed (Figure S8), had no

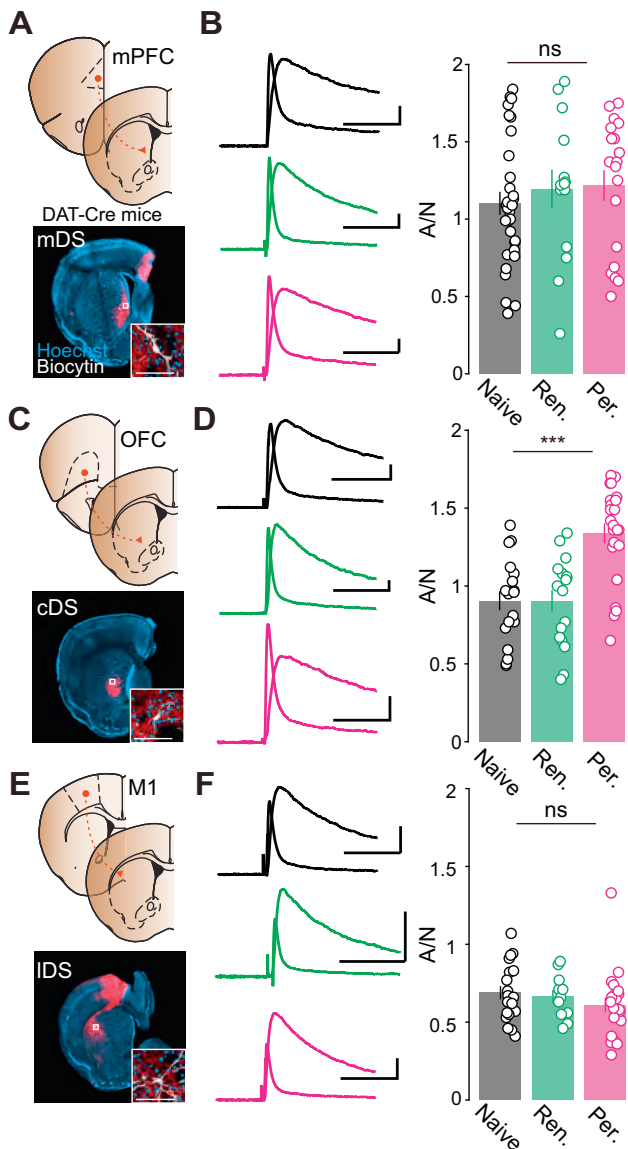


Figure 4. Potentiation of OFC-cDS synapses in persevering mice. **(A)** Schematic of the preparation for ex vivo recordings at mPFC-mDS synapses (top). Coronal section shows terminals in the striatum and recorded neuron (bottom). Inset shows recorded neuron at high magnification. **(B)** Example traces (average of 20 sweeps) of AMPA and NMDA EPSCs, recorded at +40 mV in mDS slices from naive, Ren., or Per. mice (left). A/N ratios of three groups are not statistically different (right) ($n = 31/14/19$, naive/Ren./Per., analysis of variance; $F_{2,61} = 0.4941$, $p = .62$). **(C)** Schematic of the preparation for **(D)** (top). Coronal section shows terminals in the striatum and recorded neuron (bottom). Inset shows recorded neuron at high magnification. **(D)** Example traces (average of 20 sweeps) of AMPA and NMDA EPSCs, recorded at +40 mV in cDS slices from naive, Ren., or Per. mice (left). A/N ratio is increased in Per. mice but not Ren. mice (right) ($n = 19/17/23$, naive/Ren./Per., analysis of variance; $F_{2,56} = 15.95$, $p < .0001$, post hoc comparison with Bonferroni test yielded: $p < .0001$ for naive vs. Per.; $p < .0001$ for Ren. vs. Per.). **(E)** Schematic of the preparation for **(F)** (top). Coronal section shows terminals in the striatum and recorded neuron (bottom). Inset shows recorded neuron at high magnification. **(F)** Example traces (average of 20 sweeps) of AMPA and NMDA EPSCs, recorded at +40 mV in IDS slices from naive, Ren., or Per. mice (left). A/N ratios of three groups are

impact on compulsive seeking behavior (Figure 7E, F). We conclude that brief cDS inhibition is not aversive per se but can reduce seeking behavior selectively in perseverer mice.

DISCUSSION

We observed compulsive seeking behavior in about 60% of the mice rewarded by oDASS, and we identified a selective synaptic potentiation at the OFC to SPN synapses in the DS, along with a peak in calcium activity at the moment of the seek lever retraction. Chemogenetic and optogenetic inhibition of OFC and DS neurons established that the DS SPN activity peak depends on the neuronal activity of the OFC and triggers compulsive seeking in subsequent trials.

Compulsive drug seeking in addiction is an extreme form of decision bias, where the subject continues to seek the drug reward despite the negative consequences (1,10,38). The OFC has been implicated in this behavior, based on experimental observations of compulsive reward taking (5,29). This also seems plausible because one of the physiological roles of the OFC is to calculate cost-benefit or economic value (39).

Previously, we had linked potentiation at OFC-cDS synapses to compulsive reward taking (29). In this study, we found that similar synaptic plasticity is associated with compulsive reward seeking. To investigate the impact on cellular activity, we monitored calcium activity in the cDS and found an activity peak at the moment of seek lever retraction in persevering mice. This was not the case in renouncing animals or perseverers in the IDS, confirming the projection and phenotype-specific effect. When the OFC was chemogenetically silenced, the phasic calcium signal in the cDS was curbed, suggesting the necessity of OFC activity. In the previous study, we depotentiated the OFC-DS synapses, reducing the perseverance (29). Combining such optogenetic manipulation with photometry recordings and oDASS would require spectral separation for 3 fluorophores, which may become feasible soon.

Contrasting the hypothesis of a general loss of cortical control (30,40), we found that enhanced OFC to DS transmission is associated with compulsion (29). Such gain of function thus represents an appealing alternative to prevailing explanations. The enhanced activity in the DS, driven by the OFC after seek lever press followed by its retraction (a signal of trial completion that advertises reward availability), may alter the perceived cost-benefit balance of the behavior. The fact that the signal decreases under punishment risk in renouncers suggests degradation of the cue value. It is therefore likely that the activity peak codes for the reward value rather than punishment severity. In this scenario, perseverers continue to ascribe increasing reward values to drug-predictive cues while the perception of the punishment remains intact. Indeed, it has been reported that OFC encodes this integrated cue value

← not statistically different (right) ($n = 17/11/21$, naive/Ren./Per., analysis of variance; $F_{2,46} = 1.23$, $p = .30$). Scale bars = 50 ms, 200 pA, and 100 μ m. Error bars, SEM. *** $p < .001$. A/N, AMPA receptor-EPSCs to NMDA receptor-EPSCs ratio; cDS, central part of the dorsal striatum; EPSCs, excitatory postsynaptic currents; IDS, lateral part of the DS; mDS, medial part of the DS; mPFC, medial prefrontal cortex; ns, not significant; OFC, orbitofrontal cortex; Per., perseverer; Ren., renouncer.

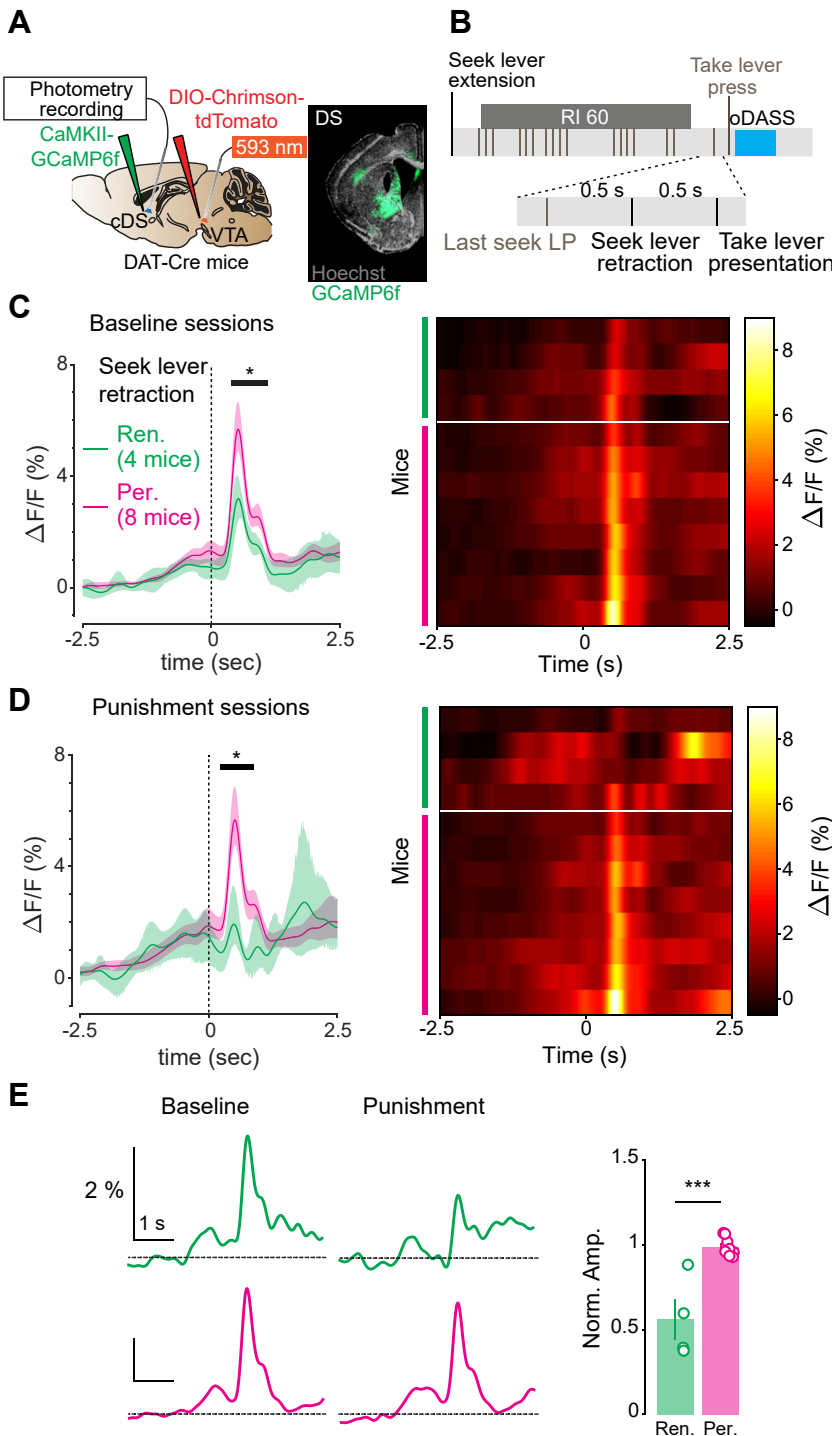


Figure 5. Activity peak in cDS neurons at seek lever retraction in persevering mice. **(A)** Schematic of the preparation for in vivo photometry recording (left), and coronal image of a mouse brain slice infected with AAV5-CaMKII-GCaMP6f in cDS (right). **(B)** Schematic for the behavioral paradigm. **(C)** Calcium signal ($\Delta F/F$) around the seek lever retraction during baseline sessions for persevering and renouncing mice (left). The black line and asterisk indicate time window with significant difference between Per. and Ren., and shaded area represents 95% confidence interval. Significant difference at 0.4361–1.0949 seconds. The heatmap shows calcium signals for an individual mouse (right). **(D)** Calcium signal ($\Delta F/F$) around the seek lever retraction during punishment sessions for persevering and renouncing mice (left). The black line and asterisk indicate time window with significant difference between Per. and Ren., and shaded area represents 95% confidence interval. Significant difference at 0.2198–0.8687 seconds. The heatmap shows calcium signals for an individual mouse (right). **(E)** Examples of calcium signals for Ren. (green) and Per. (pink) around the seek lever retraction during baseline and punishment sessions (left). Peak amplitude during punishment sessions is normalized to the amplitude during baseline sessions. Renouncers showed significant reduction of peak amplitude (right) (nonpaired two-tailed t test; $p = .0005$, $t_{10} = 5.071$). Error bars, SEM. * $p < .05$; *** $p < .001$. Amp., amplitude; cDS, central part of the dorsal striatum; LP, lever press; Norm., normalized; oDASS, optogenetic dopamine neuron self-stimulation; Per., perseverer; Ren., renouncer; RI, random interval; VTA, ventral tegmental area.

(41,42) along with the prediction of cue outcomes (43,44). Moreover, we have previously shown that perseverers and renouncers react to an unrelated painful stimulus equally (5). Our findings with reward seeking reveal a circuit that is largely overlapping with the circuit implicated in compulsive reward taking (29), underscoring the involvement of the OFC to DS

pathway across this core feature of addiction. Similar to what has been observed with compulsive oDASS or drug taking (29,45), the bimodal distribution for punishment-resistant oDASS seeking develops even in the genetically identical background of inbred animals. Moreover, the fraction of animals showing compulsive seeking for optogenetic stimulation

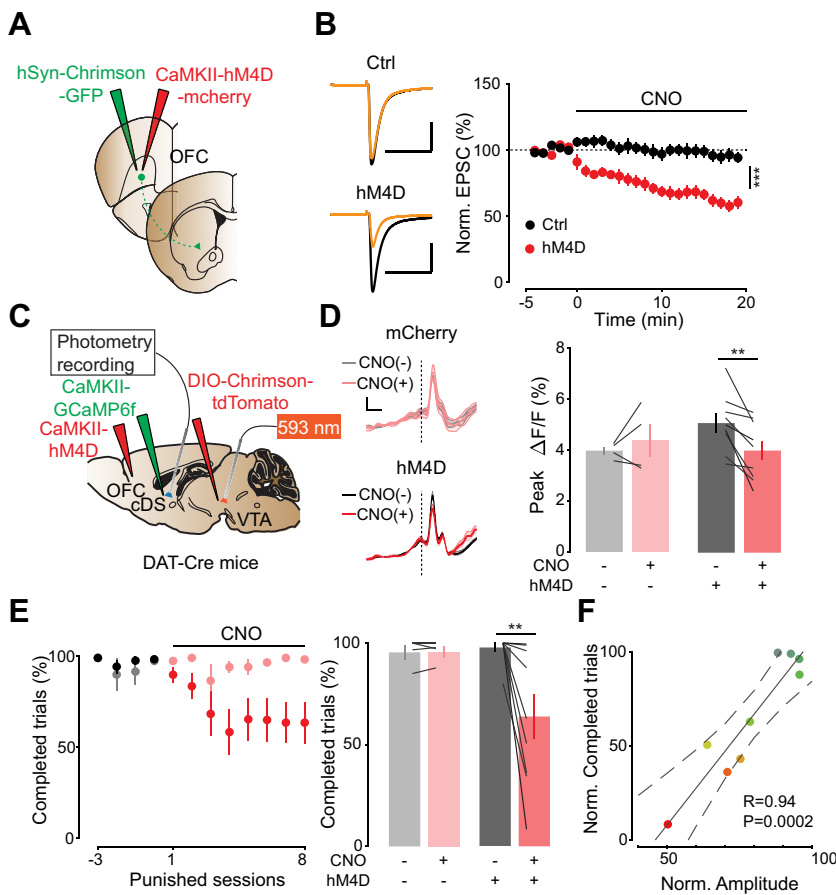


Figure 6. Reduction of compulsive reward seeking and calcium peak at seek lever retraction through chemogenetic inhibition of the OFC. **(A)** Schematic for the preparation. **(B)** Example traces of AMPA EPSCs recorded at -70 mV from control mice (top, left) and mice expressing hM4D in the OFC (bottom, left) during baseline (black) and 15 min after CNO ($10 \mu\text{M}$) bath application (yellow). Control mice received an injection of AAV9-hSyn-ChrimsonR-GFP but not AAV1-CaMKII-hM4D-mCherry. Group data for normalized EPSCs as a function of time (middle). CNO decreased light-evoked EPSCs in the cDS (nonpaired two-tailed t test, $t_{20} = 5.049$, $p < .0001$). Scale bars = 50 ms, 500 pA. Number of recorded neurons, Ctrl/hM4D; 10/12. **(C)** Schematic for the preparation. **(D)** Calcium signals around seek lever retraction before CNO injection and during CNO injection with or without hM4D expression. Shaded area represents SEM (left). CNO injection reduced peak amplitude in the experimental group but not in the control group. Mixed two-way analysis of variance: hM4D expression, $F_{1,11} = 0.3716$, $p = .5545$; CNO injection, $F_{1,11} = 1.565$, $p = .2368$; interaction, $F_{1,11} = 8.039$, $p = .0152$. Bonferroni post hoc analysis, $**p < .01$. **(E)** Percent of completed trials over sessions (left). After four sessions of punishment, CNO was injected 1 hour before each session (2 mg/kg , i.p.). Percent of completed trials on the last 2 days before CNO injection and the past 6 days during CNO injections (right). CNO injection reduced percent of completed trials in the experimental group but not in the control group, Wilcoxon matched pairs signed-rank test. p value was adjusted with Bonferroni-Dunn method. $**p < .01$. **(F)** Normalized calcium signal amplitude (before CNO/during CNO) as a function of normalized completed trials (before CNO/during CNO). Only mice with hM4D expression in the OFC are shown.

Two parameters are positively correlated (Pearson correlation coefficient $R = 0.938$, $p = .00019$). The colors in the scatter plot identify the injection sites shown in Figure S12. Error bars, SEM. $**p < .01$; $***p < .001$. cDS, central part of the dorsal striatum; CNO, clozapine N-oxide; Ctrl, control; EPSC, excitatory postsynaptic current; i.p., intraperitoneal; Norm., normalized; OFC, orbitofrontal cortex; VTA, ventral tegmental area.

of VTA DA neurons (approximately 60%) using the seek-take chain schedule is very similar to what was previously determined with a simpler version of the oDASS compulsive taking task (29). Altogether, these data suggest that vulnerability to compulsive oDASS seeking and taking involves the overlapping neural substrate of potentiated OFC-cDS transmission.

We did not find alterations in mPFC to mDS or M1 to IDS projections. This does not preclude a concomitant role of the prelimbic in compulsion (30) via reduced behavioral inhibition. For example, the prelimbic to NAc pathway is involved in compulsive reward taking (31). Afferents onto SPNs of the IDS, which is the major target of the projection from M1, remained unchanged with our paradigm. Because the latter has been implicated in habitual responding in drug self-administration protocols, our findings do not provide evidence that compulsive seeking arises from a failure to disengage from habitual performance (32).

In this study, we used compulsive oDASS seeking as an addiction model. This has the advantage of a very selective intervention with high temporal precision, minimizing off-target effects typical of pharmacological substances. However, there

is already experimental support for the involvement of the OFC-DS pathway in other models of drug-adaptive behavior. Specifically, acute injection of cocaine activates the OFC-DS pathway and induces synaptic potentiation (36,46). After short withdrawal, the synaptic transmission between the OFC and DS is stronger than in basal conditions (9). During cue-induced craving, the OFC is hyperactive in rodents (47) and human patients with substance use disorders (48). These data suggest that the potentiation at the OFC-DS pathway drives drug-seeking behavior when the OFC becomes hyperactive in response to drug-associated cues. With the introduction of a punishment risk, this OFC-DS hyperfunction is maintained only in compulsive animals. In contrast, it has been reported that the OFC is hypoactive in addicted patients (49) or rodents after cocaine self-administration (50). However, in these studies, OFC activity was measured only after long withdrawal without any drug-related cue presentation, which does not contradict a model of gain of function of the OFC in addiction. Previously, it has been demonstrated that oDASS evokes similar neuronal adaptations as cocaine (5). Here, we observed robust cue-induced reinstatement behavior (Figure S3), which is an established model of relapse (34,35), suggesting that oDASS

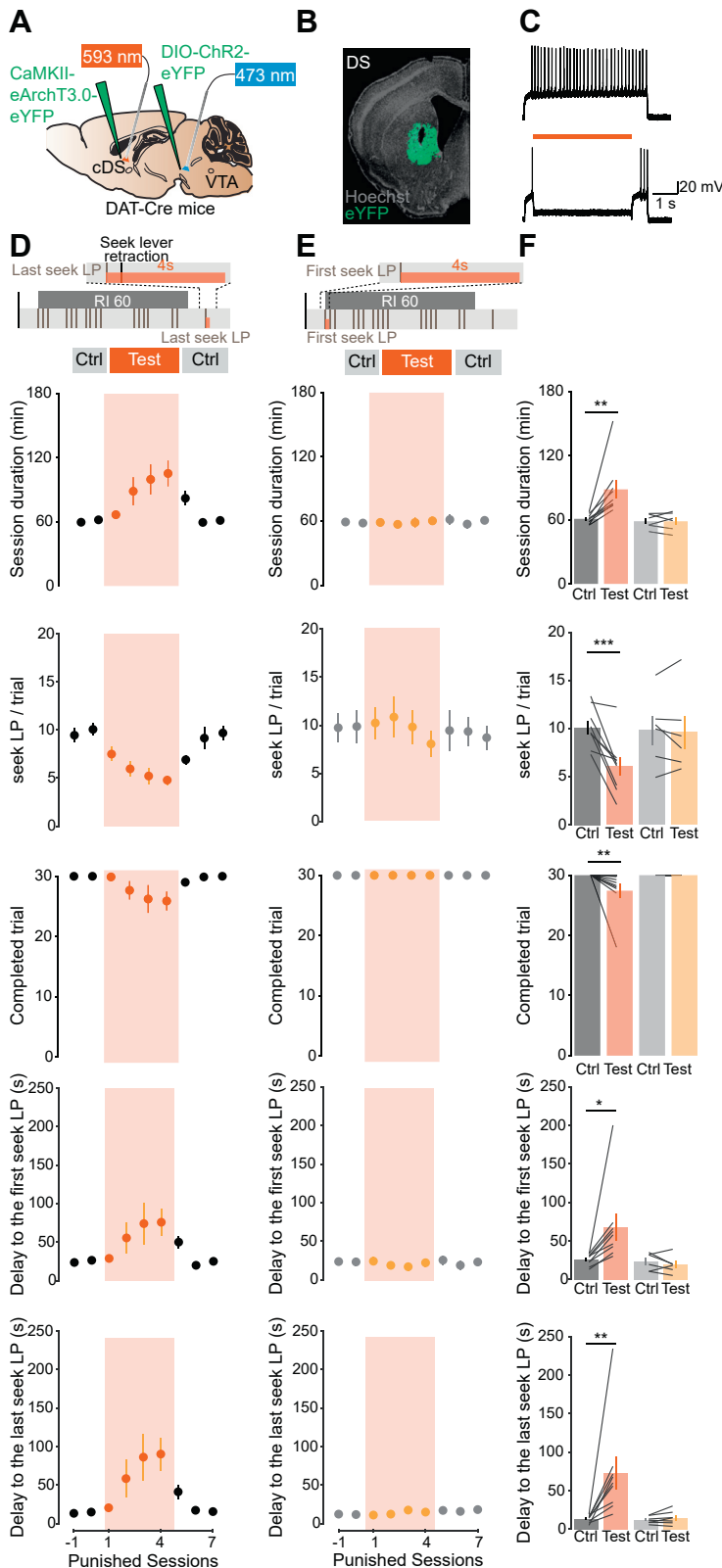


Figure 7. Reduction of compulsive reward seeking by time-locked optogenetic inhibition of cDS neurons. **(A)** Schematic for the preparation. **(B)** Image of a mouse brain infected with eArchT3.0-eYFP in the cDS. **(C)** Orange light (593 nm) suppressed action potentials induced by current injections (300 pA, 5 s) in eArchT3.0 expressing neurons. **(D)** Schematic for the inhibition protocol (top). Five parameters used for the clustering in **Figure 1F** (bottom). **(E)** Schematic for the inhibition protocol (top), same parameters as in **(D)** (bottom). **(F)** Group data for **(D)** and **(E)**. Behavior was modified by the inhibition at the moment of the last seek LP but not the first seek LP. The average of 2 sessions before inhibition (session -1 and 0) and the last 3 days of inhibition (session 2-4) are shown as Ctrl and Test, respectively. Session duration; mixed two-way ANOVA: laser timing, $F_{1,13} = 6.542, p = .0238$; treatment, $F_{1,13} = 7.603, p = .0163$; interaction, $F_{1,13} = 7.638, p = .0161$. Bonferroni post hoc analysis, $**p < .01$. Number of seek lever presses per trial; mixed two-way ANOVA: laser timing, $F_{1,13} = 1.098, p = .3138$; treatment, $F_{1,13} = 15.08, p = .0019$; interaction, $F_{1,13} = 12.00, p = .0042$. Bonferroni post hoc analysis, $***p < .001$. Number of completed trials; Wilcoxon matched pairs signed-rank test. p value was adjusted with Bonferroni-Dunn method. $**p < .01$. Delay to the first seek lever press; mixed two-way ANOVA: laser timing, $F_{1,13} = 4.538, p = .0528$; treatment, $F_{1,13} = 3.696, p = .0767$; interaction, $F_{1,13} = 5.469, p = .0360$. Bonferroni post hoc analysis, $***p < .05$. Delay to the last seek lever press; mixed two-way ANOVA: laser timing, $F_{1,13} = 4.472, p = .0543$; treatment, $F_{1,13} = 6.024, p = .0290$; interaction, $F_{1,13} = 4.733, p = .0486$. Bonferroni post hoc analysis, $**p < .01$. Error bars, SEM. ANOVA, analysis of variance; cDS, central part of the dorsal striatum; Ctrl, control; LP, lever press; RI, random interval; VTA, ventral tegmental area.

could reproduce neuronal adaptations induced by addictive drugs. To test for a potential distinct role of D1 and D2 medium spiny neurons (51), future studies will have to establish mouse lines for dual conditional expression (e.g., Cre and floppase lines for the VTA and medium spiny neurons, respectively). Previously, we found that perseverers have potentiated synapses in both D1 and D2 medium spiny neurons at the OFC-DS pathway. However, in this study, where we investigated compulsive seeking instead of compulsive taking, it remains possible that specific subpopulations of neurons code for seeking and taking, respectively. Finally, a caveat as to the photometry signal is warranted. It has recently been reported that in the striatum, the photometry signal only weakly correlates with somatic activity (52). The signal observed in this study therefore may also reflect the subthreshold of synaptic activity. To parse the contribution of the neuropil to the photometry signal, endoscopic calcium activity or single-unit firing will be needed.

In summary, we identified a neural correlate of compulsive reward seeking that is expressed as enhanced synaptic transmission in corticostriatal synapses and causes a peak in neural activity in the DS at the moment of the evaluation of the integrated reward value. In renouncing mice, the reward-related activity in the DS weakens as punishment arises, likely lowering integrated reward value and thus bringing oDASS to a halt. In compulsive animals, in contrast, the neuronal activity encoding integrated reward value remains intact despite the introduction of punishment and the decision remains in favor of seeking the reward. The identification of OFC-DS neural activity driving pathological decision making could offer new circuit-based strategies for addiction therapies.

ACKNOWLEDGMENTS AND DISCLOSURES

This work was supported by grants from the Swiss National Science Foundation (Grant Nos. 310030_189188 and CRSII5_186266 [to CL]), the National Center of Competence in Research SYNAPSY-The Synaptic Bases of Mental Diseases (to CL), and an advanced grant from the European Research Council (MeSSI, F-Addict) (to CL).

MH performed patch recordings, in vivo photometry, and anatomical tracing with the help of VP. MH and AH did surgeries for viral infection and behavioral experiments. JF implemented the clustering analysis. CL supervised the work and prepared the manuscript with the help of all authors.

We thank Meaghan Creed for comments on the manuscript and C. Gerfen for providing Cre-mouse lines through the Mutant Mouse Resource & Research Centers repository.

A previous version of this article was published as a preprint on bioRxiv: <https://doi.org/10.1101/789495>.

The authors report no biomedical financial interests or potential conflicts of interest.

ARTICLE INFORMATION

From the Department of Basic Neurosciences (MH, VP, AH, JF, CL), Faculty of Medicine, University of Geneva; and the Clinic of Neurology (CL), Department of Clinical Neurosciences, Geneva University Hospital, Geneva, Switzerland.

Address correspondence to Christian Lüscher, M.D., at Christian.Luscher@unige.ch.

Received May 17, 2021; revised Jul 29, 2021; accepted Aug 27, 2021.

Supplementary material cited in this article is available online at <https://doi.org/10.1016/j.biopsych.2021.08.018>.

REFERENCES

- Lüscher C, Robbins TW, Everitt BJ (2020): The transition to compulsion in addiction. *Nat Rev Neurosci* 21:247–263.
- Anthony JC, Warner LA, Kessler RC (1994): Comparative epidemiology of dependence on tobacco, alcohol, controlled substances, and inhalants: Basic findings from the national comorbidity survey. *Exp Clin Psychopharmacol* 2:244–268.
- Pelloux Y, Dilleen R, Economidou D, Theobald D, Everitt BJ (2012): Reduced forebrain serotonin transmission is causally involved in the development of compulsive cocaine seeking in rats. *Neuropsychopharmacology* 37:2505–2514.
- Deroche-Gamonet V, Belin D, Piazza PV (2004): Evidence for addiction-like behavior in the rat. *Science* 305:1014–1017.
- Pascoli V, Terrier J, Hiver A, Lüscher C (2015): Sufficiency of mesolimbic dopamine neuron stimulation for the progression to addiction. *Neuron* 88:1054–1066.
- Pelloux Y, Murray JE, Everitt BJ (2015): Differential vulnerability to the punishment of cocaine related behaviours: Effects of locus of punishment, cocaine taking history and alternative reinforcer availability. *Psychopharmacology (Berl)* 232:125–134.
- Siciliano CA, Noamany H, Chang CJ, Brown AR, Chen X, Leible D, et al. (2019): A cortical-brainstem circuit predicts and governs compulsive alcohol drinking. *Science* 366:1008–1012.
- Kasanetz F, Deroche-Gamonet V, Berson N, Balado E, Lafourcade M, Manzoni O, Piazza PV (2010): Transition to addiction is associated with a persistent impairment in synaptic plasticity. *Science* 328:1709–1712.
- Hu Y, Salmeron BJ, Krasnova IN, Gu H, Lu H, Bonci A, et al. (2019): Compulsive drug use is associated with imbalance of orbitofrontal and prelimbic-striatal circuits in punishment-resistant individuals. *Proc Natl Acad Sci U S A* 116:9066–9071.
- Everitt BJ, Robbins TW (2016): Drug addiction: Updating actions to habits to compulsions ten years on. *Annu Rev Psychol* 67:23–50.
- Lüscher C, Ungless MA (2006): The mechanistic classification of addictive drugs. *PLoS Med* 3:e437.
- Di Chiara G, Imperato A (1988): Drugs abused by humans preferentially increase synaptic dopamine concentrations in the mesolimbic system of freely moving rats. *Proc Natl Acad Sci U S A* 85:5274–5278.
- Bockisch C, Pascoli V, Wong JCY, House DRC, Yvon C, de Roo M, et al. (2013): Cocaine disinhibits dopamine neurons by potentiation of GABA transmission in the ventral tegmental area. *Science* 341:1521–1525.
- Pascoli V, Terrier J, Espallergues J, Valjent E, O'Connor EC, Lüscher C (2014): Contrasting forms of cocaine-evoked plasticity control components of relapse. *Nature* 509:459–464.
- Pascoli V, Turiault M, Lüscher C (2011): Reversal of cocaine-evoked synaptic potentiation resets drug-induced adaptive behaviour. *Nature* 481:71–75.
- Ma YY, Lee BR, Wang X, Guo C, Liu L, Cui R, et al. (2014): Bidirectional modulation of incubation of cocaine craving by silent synapse-based remodeling of prefrontal cortex to accumbens projections. *Neuron* 83:1453–1467.
- Hearing MC, Jedynak J, Ebner SR, Ingebreton A, Asp AJ, Fischer RA, et al. (2016): Reversal of morphine-induced cell-type-specific synaptic plasticity in the nucleus accumbens shell blocks reinstatement. *Proc Natl Acad Sci U S A* 113:757–762.
- Willuhn I, Burgeno LM, Everitt BJ, Phillips PEM (2012): Hierarchical recruitment of phasic dopamine signaling in the striatum during the progression of cocaine use. *Proc Natl Acad Sci U S A* 109:20703–20708.
- Everitt BJ, Robbins TW (2013): From the ventral to the dorsal striatum: Devolving views of their roles in drug addiction. *Neurosci Biobehav Rev* 37:1946–1954.
- Zapata A, Minney VL, Shippenberg TS (2010): Shift from goal-directed to habitual cocaine seeking after prolonged experience in rats. *J Neurosci* 30:15457–15463.
- Jonkman S, Pelloux Y, Everitt BJ (2012): Differential roles of the dorsolateral and midlateral striatum in punished cocaine seeking. *J Neurosci* 32:4645–4650.

22. Balleine BW, O'Doherty JP (2010): Human and rodent homologies in action control: Corticostriatal determinants of goal-directed and habitual action. *Neuropsychopharmacology* 35:48–69.
23. Belin D, Jonkman S, Dickinson A, Robbins TW, Everitt BJ (2009): Parallel and interactive learning processes within the basal ganglia: Relevance for the understanding of addiction. *Behav Brain Res* 199:89–102.
24. Gruber AJ, McDonald RJ (2012): Context, emotion, and the strategic pursuit of goals: Interactions among multiple brain systems controlling motivated behavior. *Front Behav Neurosci* 6:50.
25. Thorn CA, Atallah H, Howe M, Graybiel AM (2010): Differential dynamics of activity changes in dorsolateral and dorsomedial striatal loops during learning. *Neuron* 66:781–795.
26. Yin HH, Knowlton BJ (2006): The role of the basal ganglia in habit formation. *Nat Rev Neurosci* 7:464–476.
27. Yin HH, Ostlund SB, Knowlton BJ, Balleine BW (2005): The role of the dorsomedial striatum in instrumental conditioning. *Eur J Neurosci* 22:513–523.
28. Hunnicutt BJ, Jongbloets BC, Birdsong WT, Gertz KJ, Zhong H, Mao T (2016): A comprehensive excitatory input map of the striatum reveals novel functional organization. *Elife* 5:e19103.
29. Pascoli V, Hiver A, Van Zessen R, Loureiro M, Achargui R, Harada M, *et al.* (2018): Stochastic synaptic plasticity underlying compulsion in a model of addiction. *Nature* 564:366–371.
30. Chen BT, Yau HJ, Hatch C, Kusumoto-Yoshida I, Cho SL, Hopf FW, Bonci A (2013): Rescuing cocaine-induced prefrontal cortex hypoactivity prevents compulsive cocaine seeking. *Nature* 496:359–362.
31. Domingo-Rodríguez L, Ruiz de Azua I, Domínguez E, Senabre E, Serra I, Kummer S, *et al.* (2020): A specific prefrontal-nucleus accumbens pathway controls resilience versus vulnerability to food addiction. *Nat Commun* 11:782.
32. Giuliano C, Belin D, Everitt BJ (2019): Compulsive alcohol seeking results from a failure to disengage dorsolateral striatal control over behavior. *J Neurosci* 39:1744–1754.
33. Brown MTC, Bellone C, Mameli M, Labouèbe G, Bocklisch C, Bolland B, *et al.* (2010): Drug-driven AMPA receptor redistribution mimicked by selective dopamine neuron stimulation. *PLoS One* 5: e15870.
34. Chen BT, Bowers MS, Martin M, Hopf FW, Guillory AM, Carelli RM, *et al.* (2008): Cocaine but not natural reward self-administration nor passive cocaine infusion produces persistent LTP in the VTA. *Neuron* 59:288–297.
35. Roberts-Wolfe D, Bobadilla AC, Heinsbroek JA, Neuhof D, Kalivas PW (2018): Drug refraining and seeking potentiate synapses on distinct populations of accumbens medium spiny neurons. *J Neurosci* 38:7100–7107.
36. Bariselli S, Miyazaki NL, Creed MC, Kravitz AV (2020): Orbitofrontal-striatal potentiation underlies cocaine-induced hyperactivity. *Nat Commun* 11:3996.
37. Stachniak TJ, Ghosh A, Sternson SM (2014): Chemogenetic synaptic silencing of neural circuits localizes a hypothalamus→midbrain pathway for feeding behavior. *Neuron* 82:797–808.
38. Nestler EJ, Lüscher C (2019): The molecular basis of drug addiction: Linking epigenetic to synaptic and circuit mechanisms. *Neuron* 102:48–59.
39. Padoa-Schioppa C, Assad JA (2006): Neurons in the orbitofrontal cortex encode economic value. *Nature* 441:223–226.
40. Goldstein RZ, Volkow ND (2011): Dysfunction of the prefrontal cortex in addiction: Neuroimaging findings and clinical implications. *Nat Rev Neurosci* 12:652–669.
41. Hirokawa J, Vaughan A, Masset P, Ott T, Kepecs A (2019): Frontal cortex neuron types categorically encode single decision variables. *Nature* 576:446–451.
42. Masset P, Ott T, Lak A, Hirokawa J, Kepecs A (2020): Behavior- and modality-general representation of confidence in orbitofrontal cortex. *Cell* 182:112–126.e18.
43. Schoenbaum G, Chang CY, Lucantonio F, Takahashi YK (2016): Thinking outside the box: Orbitofrontal cortex, imagination, and how we can treat addiction. *Neuropsychopharmacology* 41:2966–2976.
44. Takahashi YK, Chang CY, Lucantonio F, Haney RZ, Berg BA, Yau HJ, *et al.* (2013): Neural estimates of imagined outcomes in the orbitofrontal cortex drive behavior and learning. *Neuron* 80:507–518.
45. Belin D, Berson N, Balado E, Piazza PV, Deroche-Gamonet V (2011): High-novelty-preference rats are predisposed to compulsive cocaine self-administration. *Neuropsychopharmacology* 36:569–579.
46. Wall NR, Neumann PA, Beier KT, Mokhtari AK, Luo L, Malenka RC (2019): Complementary genetic targeting and monosynaptic input mapping reveal recruitment and refinement of distributed corticostriatal ensembles by cocaine. *Neuron* 104:916–930.e5.
47. Fanous S, Goldart EM, Theberge FRM, Bossert JM, Shaham Y, Hope BT (2012): Role of orbitofrontal cortex neuronal ensembles in the expression of incubation of heroin craving. *J Neurosci* 32:11600–11609.
48. Bonson KR, Grant SJ, Contoreggi CS, Links JM, Metcalfe J, Weyl HL, *et al.* (2002): Neural systems and cue-induced cocaine craving. *Neuropsychopharmacology* 26:376–386.
49. Volkow ND, Wang GJ, Fowler JS, Tomasi D, Telang F (2011): Addiction: Beyond dopamine reward circuitry. *Proc Natl Acad Sci U S A* 108:15037–15042.
50. Lucantonio F, Stalnaker TA, Shaham Y, Niv Y, Schoenbaum G (2012): The impact of orbitofrontal dysfunction on cocaine addiction. *Nat Neurosci* 15:358–366.
51. Kravitz AV, Tye LD, Kreitzer AC (2012): Distinct roles for direct and indirect pathway striatal neurons in reinforcement. *Nat Neurosci* 15:816–818.
52. Legaria AA, Licholai JA, Kravitz AV (2021): Fiber photometry does not reflect spiking activity in the striatum. *bioRxiv*. <https://doi.org/10.1101/2021.01.20.427525>.